Rates of attachment of fibroblasts to self-assembled monolayers formed by the adsorption of alkylthiols onto gold surfaces

Elaine Cooper,[a] Robin Wiggs,[b] David A. Hutt,[a] Lesley Parker,[b] Graham J. Leggett*[a†] and Terry L. Parker[b]

Departments of [a]Materials Engineering and Materials Design and [b]Human Morphology, The University of Nottingham, University Park, Nottingham, UK NG7 2RD

Self-assembled monolayers (SAMs) of alkylthiols on gold surfaces have been prepared and characterised by contact angle goniometry and X-ray photoelectron spectroscopy. Murine 3T3 fibroblasts were cultured on single-component monolayers of adsorbates with carboxylic acid and methyl termini, and the rates of cellular attachment measured over 90 minutes. Cell attachment was found to be approximately twice as rapid for carboxylic acid-terminated monolayers as for methyl-terminated monolayers. After 24 hours, substantially greater numbers of 3T3 cells were found to be attached to the hydrophilic monolayers than were attached to the hydrophobic ones. Murine 3T3 cells were also cultured on patterned SAMs which were prepared using UV photochemistry and characterised using scanning electron microscopy. The cells attached exclusively to the acid-functionalised areas of the patterned surface, leaving the methyl-functionalised regions bare. The patterns also strongly influenced the morphology of the attached cells.

The phenomena of cellular attachment and adhesion onto solid surfaces are of importance both for fundamental studies of cell growth and function and for technological applications which utilise cellular structures, including the development of novel prosthetic materials, nerve regeneration and bioelectronics and biosensors. Cell–surface interactions remain complex and poorly understood, largely because of the vast diversity of processes and parameters which control them. Both the microtopography and the surface chemistry of the substratum are known to exert an influence over cell–surface interactions. Surface chemistry is known to influence cellular adhesion, but in a serum-containing medium, the substratum is likely to become covered with adsorbed proteins prior to cell attachment. The influence of surface chemistry is thus convoluted by the structure of the adsorbed protein layer which forms upon exposure to the cell culture medium. Indirectly, cellular adhesion is influenced *via* the conformational changes which occur in the proteins as they adsorb to the substratum and which are determined by the surface chemistry of the substratum.

The design of suitable experiments by which to investigate the processes of cellular attachment and adhesion is therefore a formidable scientific challenge, and no single experimental system will enable all of the relevant parameters to be defined and examined. Rather, it is necessary to devise a specific experimental milieu in which the influence of particular parameters may be explored. Recent examples include the utilisation of lithographically engineered micro-morphologies to examine cellular guidance by ultrafine topography[1–3] and the exploration of specific chemistries, including polymeric films,[4,5] adsorbed layers of cell-adhesive proteins[6] and monolayers of adsorbed organic molecules,[7–14] on solid supports. Recent years have seen substantial interest in the utilisation of self-assembled monolayers (SAMs), formed typically by the chemisorption of alkylthiols onto gold surfaces[15–17] or by the chemisorption of alkylsilanes onto silica surfaces,[18] to model a variety of interfacial phenomena including wetting,[19–23] adhesion,[24–26] molecular recognition[27–30] and biological interactions.[7,8,12–14,31–33] We are interested in using SAMs as model materials in systematic studies of cell–surface interactions. The objective of our research is to determine the surface chemical controls over cellular attachment and adhesion on solid surfaces, and to explore the potential utility of SAMs as templates for the fabrication of novel cellular devices and structures.

Prime and Whitesides[31] have shown that self-assembled monolayers formed by the coadsorption of mixed monolayers of ω-terminated alkylthiols on gold may be employed as model substrates in studies of protein adsorption. The feasibility of culturing cells on SAMs formed by the adsorption of alkylthiols on gold has also been demonstrated.[13,14] Rat basophilic leukaemia cells were found to attach to SAMs with a variety of different surface chemistries, including monolayers with tertiary amine, carboxylic acid, methyl and perfluorinated tail groups, although the numbers of attached cells varied to some (unquantified) extent with surface chemistry.[13] In contrast, SAMs terminated with oligo(ethylene glycol) groups proved non-adhesive to cells. MG63 osteosarcoma cells exhibited different behaviour, and were observed to attach preferentially to hydroxy-terminated SAMs, but not to adjacent methyl-terminated SAMs indicating a strong dependence on SAM surface energy.[14] Predominantly, however, published studies have employed silane monolayers on silicon substrates. Stenger and co-workers have studied neuronal attachment to amino and perfluorinated alkylsilanes, and by utilising UV photochemistry have prepared patterned materials for the spatial definition of cell growth.[10,11] In a systematic study, Lewandowska *et al.* studied cell and protein interactions with alkylsilanes with a variety of tail functionalities, utilising radiolabelling techniques to assay amounts of adsorbed protein, and examining actin stress fibre organisation by phase contrast microscopy.[7,8]

In the present study the influence of surface chemistry on the rate of attachment of substrate-dependent 3T3 murine fibroblasts has been explored. Single-component alkylthiol-on-gold SAMs have been prepared from adsorbates with methyl [octanethiol (OT)] and carboxylic acid [3-mercaptopropanoic acid (MPA)] tail groups and rates of attachments of cells have been investigated over 90 min. In addition, cell morphology for the 3T3s cultured on the SAMs with different surface chemistries has been examined by optical microscopy. Patterned monolayers of OT and MPA have also been created using UV photochemistry and murine 3T3 fibroblasts have been cultured on these monolayers. A particular advantage of this photolithographic method of patterning SAMs is that possible topographical influences on cell attachment are avoided.

† Email: Graham.Leggett@Nottingham.ac.uk

Experimental

Preparation of SAMs

Two different glass substrates were used to prepare the monolayers. The single-component monolayers were prepared on 19 mm diameter glass coverslips which were cleaned by immersion in 5 mol dm^{-3} nitric acid for 2 h followed by sonication in distilled water and drying by heating at 70 °C for several hours. The staining racks used to support the coverslips were cleaned in a similar manner. Rectangular (Chance 22×64 mm^2, no. 2 thickness) cover slips were used for the patterned monolayers. In this instance all glassware used in the sample preparation was cleaned by soaking in hot (*ca.* 90 °C) 'Piranha' solution (mixture of 30% H_2O_2 solution and conc. H_2SO_4 in a ratio of 3 : 7) then rinsed with copious amounts of distilled water and dried in an oven. Care was exercised in the use of both nitric acid and 'Piranha' solution, which may, under certain circumstances, react violently with organic material. After they had been cleaned, the different glass substrates were treated in the same way.

Monolayers of MPA and OT were prepared on evaporated gold (Goodfellow, 99.99 + %) films supported on chromium (Goodfellow, 99.99 + %) primed glass substrates. The thickness of the gold films was in the range 20–40 nm and the gold was deposited at a rate of *ca.* 0.5 Å s^{-1}. Samples prepared within this range of thickness were optically transparent and examination of cells by optical microscopy was not impeded by the presence of the gold film. Following deposition of the gold film, samples were immersed in 1 mmol dm^{-3} solutions of the thiols in degassed ethanol for 12–18 h. The time interval between removal of the samples from the evaporator and their immersion in the thiol solution was typically less than 4 min. Following removal of samples from the adsorbate solution, they were rinsed with degassed ethanol and dried under a stream of nitrogen. OT (97%) was obtained from Fluka, and was used as received. MPA (99%) was obtained from Aldrich and also used as received.

The patterned monolayers were created using a modified version of the photolithographic process of Tarlov and coworkers,[34,35] employing transmission electron microscope grids (Agar) as masks to create micron-scale features on the surface. UV irradiation of alkylthiol-on-gold SAMs in the presence of air results in the photo-oxidation of the alkylthiolate adsorbate complex to yield an alkylsulfonate. The weakness of the SO_3–Au interaction facilitates the displacement of the alkylsulfonate by a second thiol adsorbed from solution, resulting in the formation of a new SAM on the UV-exposed areas. In this study several electron microscope grids were placed directly on a freshly prepared MPA SAM which was then placed under a medium-pressure mercury arc UV lamp for 60 min. The grids were removed and the samples were then immersed in a freshly prepared 1 mmol dm^{-3} OT solution for 7 min after which they were taken out of solution, rinsed with degassed ethanol and dried with N_2 gas. The resulting monolayers were hydrophobic in the exposed regions while the masked regions remained hydrophilic. Grids with a variety of geometries and dimensions were used to investigate whether feature dimensions had a role to play in influencing the growth of cells on the patterned surface.

The purity of the single component monolayers was assessed by X-ray photoelectron spectroscopy (XPS) and the wettability was measured by contact angle goniometry. XPS measurements were performed using a VG ESCALab system equipped with a twin anode X-ray source and a 100 mm radius hemispherical electron energy analyser. The sampled area was *ca.* 9 mm in diameter and the take-off angle was 70°. Mg-Kα radiation was employed, with the sample held at maximum separation from the X-ray source in order to minimise damage. Advancing contact angles were measured using the sessile drop method (after Bain *et al.*[17]) on a Rame-Hart model 100-00 contact angle goniometer. A 2 µl droplet of water was suspended from the tip of a microlitre syringe supported above the sample stage. The syringe tip was advanced towards the sample until the droplet made contact with the sample surface. The syringe was then retracted leaving the droplet on the sample. A sample was said to be wetting if the contact angle was less than 10° and the drop perimeter was observed to be deformed. The patterned monolayers were characterised using scanning electron microscopy (SEM). The SEM images were acquired in the secondary electron detection mode using a JEOL JSM-6400 scanning microscope (chamber pressure 5×10^{-6} Torr), with a 35 kV primary electron beam and a current of 3 nA. The electron detector was operated with a collection voltage of +300 V.

Cell culture

An anchorage-dependent murine fibroblastic cell line (3T3-L1) was maintained in minimum essential medium supplemented with 10% newborn calf serum, 1 mg ml^{-1} penicillin, 1 mg ml^{-1} streptomycin, 0.2% $NaHCO_3$ and 2 mmol dm^{-3} L-glutamine, and routinely subcultured by trypsinisation (0.25% trypsin in EDTA in Ca^{2+}/Mg^{2+}-free phosphate-buffered saline).

Substrates were seeded with fibroblasts in 3 ml full culture medium (FCM) at a concentration of 10^5 cells ml^{-1}, and cultured in humidified air with 5% CO_2 at 37 °C and pH 7.2.

For cell attachment assays, coverslips were dipped briefly in Earle's balanced salt solution (EBSS; pH 7.2–7.4), fixed *in situ* with 5% acetic acid in ethanol, and counted by means of systematic random sampling using a computer-based image analysis system connected to a video microscope.

Results

Characterisation of SAMs

Single-component self-assembled monolayers of OT and MPA on gold were characterised by X-ray photoelectron spectroscopy and contact angle goniometry.

Fig. 1 shows the relevant regions of the XP spectra recorded for the as-prepared SAMs of OT and MPA. With the exception of the fitted C 1s region of the MPA spectrum, the spectra are shown as recorded with no binding energy or background corrections made. For the OT SAM the C 1s peak at 285 eV is symmetrical with a full width at half maximum height (FWHM) of *ca.* 1.4 eV, indicating a single environment for the C atoms in the SAM [Fig. 1(*a*)]. The O 1s/Au $4p_{3/2}$ region of the OT spectrum is shown in Fig. 1(*b*). The Au $4p_{3/2}$ peak at 546 eV can be seen, but there is no contribution to the spectrum from O indicating that the monolayers are oxygen free. There is a broad peak at 162–163 eV in the S 2p region of the spectrum which consists of two unresolved components, the $2p_{3/2}$ and $2p_{1/2}$ [Fig. 1(*c*)].

For the MPA monolayer three peaks are observed in the C 1s region of the XP spectrum [Fig. 1(*a*)]. The peak at 285 eV is assigned to the methylene carbon atom attached to the sulfur, the peak at 287 eV to the other methylenic carbon atom and the peak at 289 eV to the carboxylic acid carbon atom. The observed peak shifts of 2 and 4 eV, compared to the standard methylene peak at 285 eV, for the middle and carboxylic carbon atoms respectively, are similar to those reported in the literature for the different carbon environments.[17] However, the observed peak area ratios for the three different carbon atoms are unexpected; all three C 1s peaks for MPA should have the same area. Clearly this is not the case as the peak assigned to the methylenic carbon attached to the sulfur has a much larger area than the other two C 1s peaks which have approximately the expected peak area ratio of 1 : 1. The discrepancy may be explained by considering that the high surface energy of the acid-terminated SAM makes it very

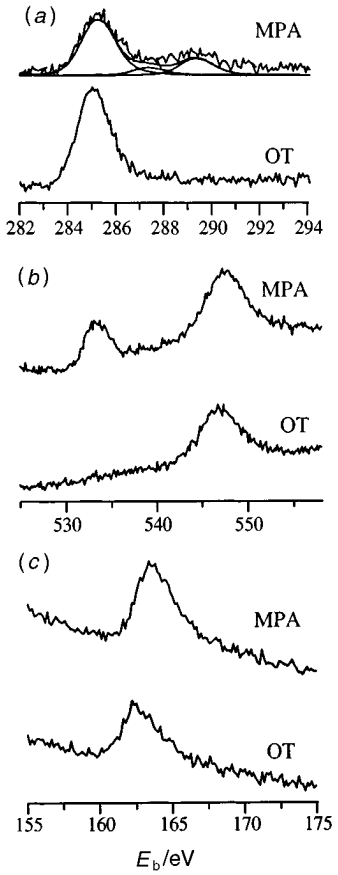

Fig. 1 XP spectra of OT and MPA SAMs: (*a*) C 1s; (*b*) O 1s/Au $4p_{3/2}$; (*c*) S 2p

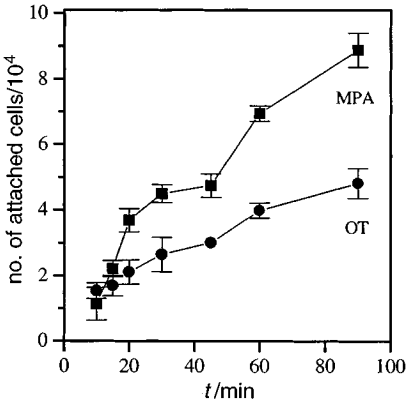

Fig. 2 Variation in the number of attached fibroblasts with time for MPA and OT monolayers

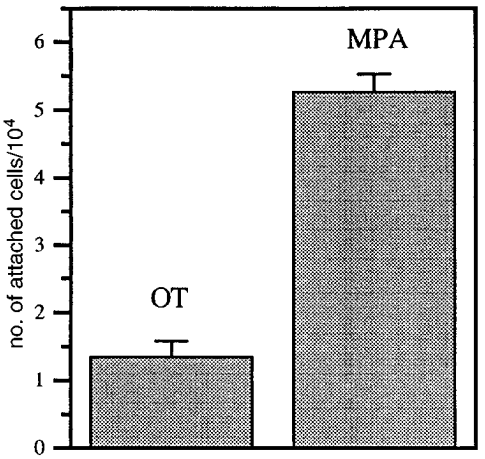

Fig. 3 Variation in the number of attached fibroblasts after 24 h for MPA and OT monolayers

susceptible to contamination from airborne molecules giving rise to the enhanced area of the peak at 285 eV. This enhanced hydrocarbon signal has been observed previously in the high-resolution XP spectra of carboxylic acid polymers where it was similarly attributed to adventitious hydrocarbon contamination resulting from the high surface energy of the polymers.[36] The oxygen and sulfur regions of the XP spectra of MPA are shown in Fig. 1(*b*) and (*c*), respectively.

Advancing contact angles of $<10^\circ$ were recorded for the single-component MPA SAMs and angles of $109\pm2^\circ$ were recorded for the single-component OT SAMs. These values agree well with the published literature.[17]

Cell culture on single-component monolayers

Rates of attachment of 3T3 murine fibroblasts for single-component monolayers of both MPA and OT were measured over 90 min (Fig. 2). Initially, the number of cells attached to the COOH-terminated monolayer was found to rise more rapidly than the number attached to the CH_3-terminated monolayer, with approximately twice as many cells attaching to the wetting surface after 20 min. Thereafter, the number of 3T3 cells attached to the MPA monolayer remained approximately twice that attached to the OT monolayer. After 24 h there are four times as many cells attached to the MPA monolayer as the OT monolayer (Fig. 3). The 3T3 cells thus exhibited a clear preference for the COOH-terminated monolayer as compared to the CH_3-terminated monolayer.

Examination of cell morphology by light microscopy after 24 h emphasised the extent of this preference. Not only were the numbers of cells greater for the wetting surface, but the morphology was strongly indicative of successful adhesion and growth. Micrographs of OT monolayers following 24 h cell culture revealed clusters of closely packed cells. Predominantly, the cells were found to be spread poorly, even where single cells were observed. Fig. 4(*a*) shows a light micrograph of 3T3 cells attached to a region of an OT SAM adjoining an exposed region of the glass cover slip masked during evaporation of the gold film. On the glass surface, the cells exhibit a more even distribution across the surface and there appears to be substantial cytoplasmic spreading. The contrast with the morphology of attached cells on the OT monolayers is marked.

Fig. 4(*b*) shows a light micrograph of an MPA monolayer following cell culture. The morphology of the attached cells is very similar to that observed for the glass substratum; cells are evenly distributed with no close-packed clusters. There is also considerable cytoplasmic spreading.

Photopatterning

The patterned SAMs were characterised using SEM and Fig. 5 shows typical SEM images recorded for different patterned monolayers. Light contrast is observed in the OT regions of the surface and dark in the MPA regions. The dark contrast in the wetting regions is thought to arise from the higher energy hydrophilic surface spontaneously adsorbing airborne molecules which attenuate the secondary electron signal arising from the gold.[37,38] The SEM images highlight the clear transition between hydrophobic and hydrophilic regions on the surface. Advancing water droplet contact angle measurements were also performed to determine differences in wettability between photopatterned regions. The masked MPA areas of the surface remained highly hydrophilic ($\theta_a<15^\circ$), while the refunctionalised OT areas gave a contact angle of *ca.* 100°. This slightly lower than expected OT contact angle (literature value 110°)[17] is a result of incomplete ordering in the SAM, due to the necessarily short exposure time of the photo-

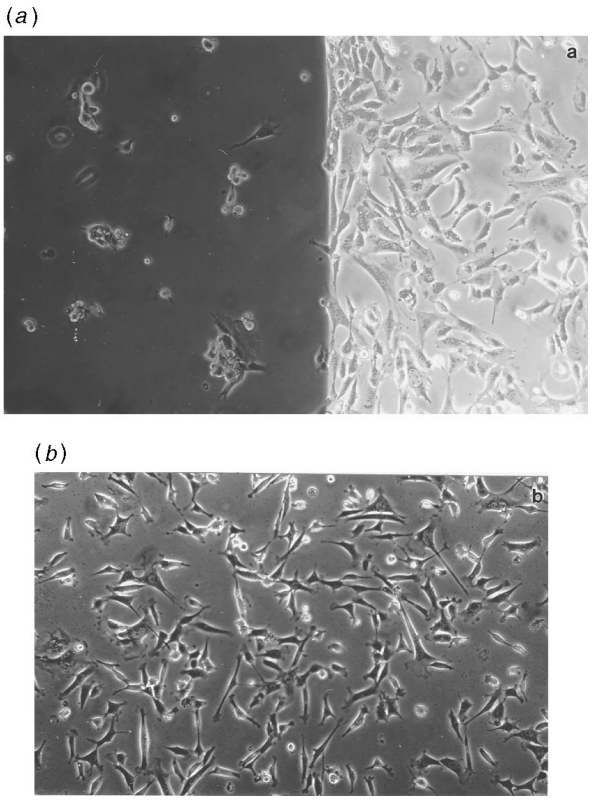

Fig. 4 Light micrographs of fibroblasts attached to (*a*) an OT monolayer (left) and glass (right) and (*b*) an MPA monolayer

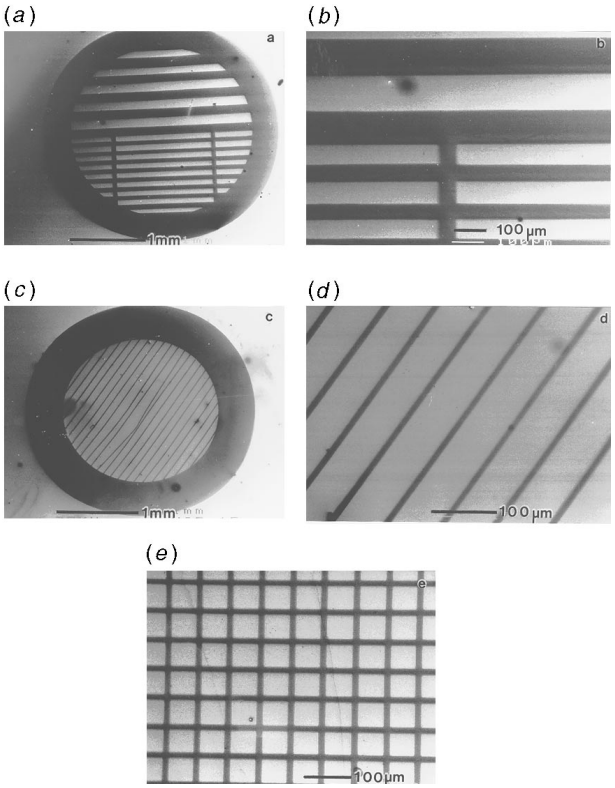

Fig. 5 SEM images of different patterned monolayers: (*a*) and (*b*) 'Sjostrand' patterned substrate; (*c*) and (*d*) 'Robertson' patterned substrate; and (*e*) '400 grid' patterned substrate

oxidised surface to the OT solution to prevent replacement of the unoxidised MPA by octanethiol. Three different masks are shown in Fig. 5: the 'Sjostrand', Fig. 5(*a*) and (*b*), 'Robertson', Fig. 5(*c*) and (*d*), and '400 grid', Fig. 5(*e*), TEM grids. The Sjostrand grid has two different bar (and slot) widths of 50 µm and 110 µm, the Robertson bar width is 15 µm with 85 µm wide slots and the bars of the grid are 11 µm wide. The overall diameter of each of the grids is 3 mm. The images observed demonstrate that the spatial separation of the MPA and OT regions corresponds to the dimensions of the TEM grids.

Cell culture on patterned substrates

Fig. 6 shows a series of light micrographs of a Sjostrand patterned substrate following 24 h of 3T3 cell culture. Comparing the light micrographs of the cells to the SEM images obtained for the same patterned surfaces [Fig. 5(*a*) and (*b*)], it is apparent that the cells enjoy a significant interaction with the hydrophilic areas of the surface, but not with the hydrophobic regions. Some cells have attached to the OT areas, but they are vastly reduced in number and also appear to be attached to cells anchored to the hydrophilic regions of the pattern. After 24 h cells start to extend in large numbers from the MPA regions onto the OT regions within the pattern due to lack of surface area available within the MPA areas. The pattern is masked after 36 h cell culture, *i.e.* the cells are confluent across the patterned region giving rise to a 'disc' of cells. However, cells on OT regions appear to be stabilised by cell–cell contacts with cells on the MPA areas. The patterned substrates demonstrate clearly that given the choice between

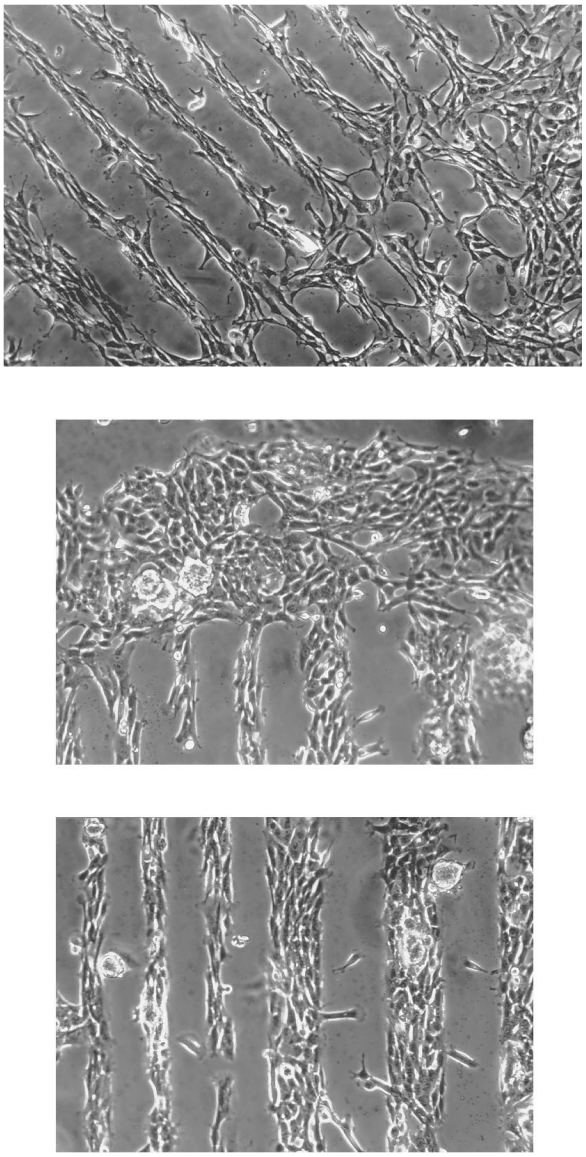

Fig. 6 Light micrographs of a Sjostrand patterned substrate following 24 h cell culture

two surfaces there is a strong preference for the 3T3 cells to interact with the carboxylic acid chemistry.

The patterned substrate can also influence strongly the morphology of the attached cells as demonstrated by the optical micrograph obtained following cell culture on patterns produced using the Robertson mask (Fig. 7). On this surface the cells conform precisely to the geometry of the patterned region and have only extended in the direction of the MPA lines on the surface, forming wire-like structures. The preference of the fibroblasts for the MPA-functionalised regions (as compared to the hydrophobic regions) has thus forced them to spread in a fashion not observed on unpatterned MPA surfaces.

Cell culture on the 400 grid patterned substrate emphasises the influence that the pattern dimensions and geometry have on the morphology of the attached cells (Fig. 8). While the complete pattern has not been exposed as it was for the other two patterns, Fig. 8 shows that a grid pattern is beginning to form. Significantly, the cell nuclei are mainly attached to the point of intersection of the grid lines with cell extension occurring only in the direction of the bars. The intersection presents the largest surface area for cell body attachment and the cell is imobilised at this point by tension in the four directions of the grid lines.

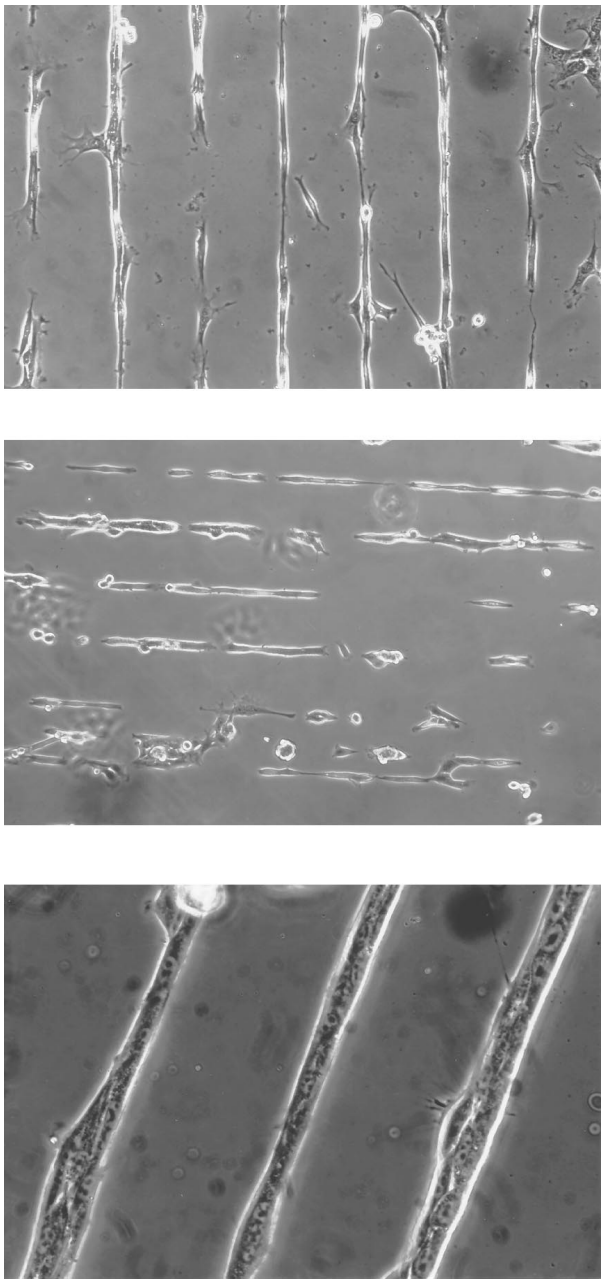

Fig. 7 Light micrographs of a Robertson patterned substrate following 24 h cell culture

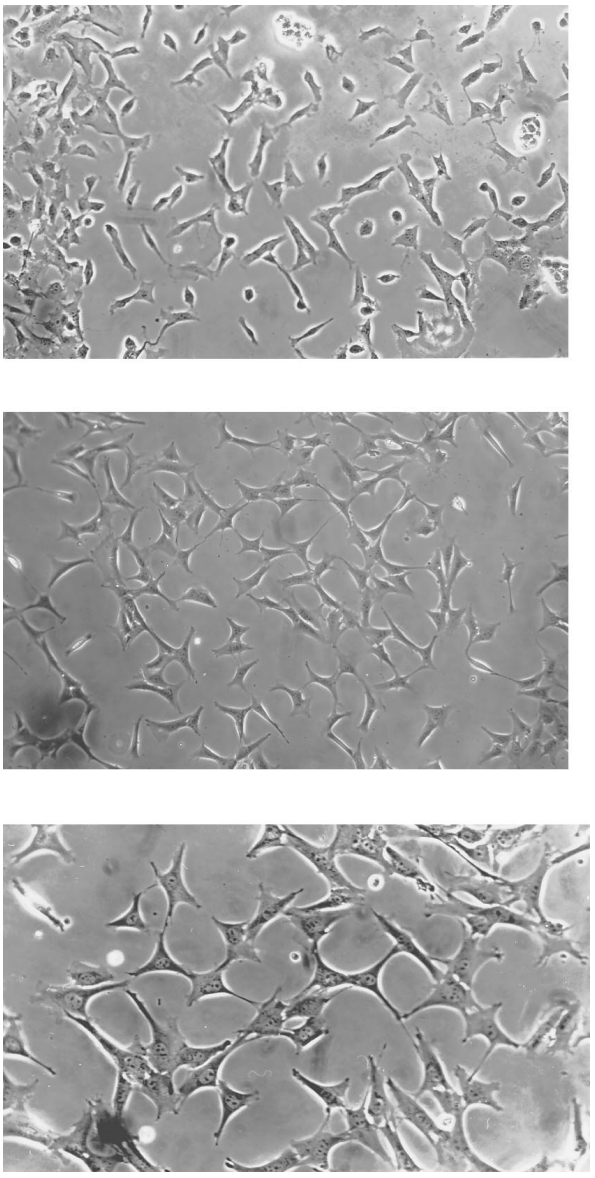

Fig. 8 Light micrographs of a '400 grid' patterned substrate following 24 h cell culture

Discussion

3T3 murine fibroblasts were cultured successfully on SAMs formed by the adsorption of acid- and methyl-functionalised alkylthiols on gold surfaces. In addition to attaching to the COOH-terminated monolayers in greater numbers, the cells also exhibited a more well spread morphology on these surfaces. In contrast, on the CH_3-terminated monolayer, the cells were poorly spread and clumped together. During the first 90 min, twice as many cells were attached to the MPA monolayers as were attached to the OT monolayers; however, after 24 h, four times as many cells were found to have attached to the COOH-functionalised monolayers. It is possible that this difference is in part a consequence of mitotic cell division on the MPA-functionalised regions and/or inhibition of cell division on the OT-functionalised regions. For the patterned monolayers the preference for the 3T3 cells to grow on the carboxylic acid-functionalised regions of the surface was very marked. This is attributed to migration of the cells to the preferred areas of the monolayer with time; an extracellular matrix (ECM) is

produced which enables the cells to migrate towards the MPA surface. Importantly, the materials also exhibited great stability over long exposures to biological media.

The influence of surface energy (or wettability) on cell attachment has been studied by a number of workers.[7,8,10,11,39] For example, Lewandowska and co-workers prepared monolayers of ω-functionalised alkylsilanes on glass, and compared the attachment of 3T3 fibroblasts to monolayers with a variety of tail functionalities, including CH_3 and COOH groups.[7,8] After 1 h, they observed little difference in numbers of fibroblasts attached to COOH- and CH_3-terminated monolayers. This result is at variance with our observations. However, Lewandowska and co-workers[7,8] recorded an advancing contact angle of 52° for the COOH-terminated monolayers compared to our value of $<10°$ for MPA monolayers. Research in this laboratory using mixed monolayers of MPA and OT suggests that substantial differences in cellular interactions may be expected for materials that exhibit a difference in surface energy of this magnitude.[40] The high contact angles reported by Lewandowska and co-workers[7,8] may be indicative of surface contamination; however, the lowest reported advancing contact angle for the acid-terminated alkylsilane-on-silica system is *ca.* 30° (for permanganate periodate oxidised vinyl-terminated monolayers),[18] indicating surface energies significantly lower than those attainable for ω-functionalised alkylthiols on gold. The measured wettability depends on adsorbate structure and ordering and also on the method used to prepare the terminal functional group. Wasserman *et al.* attributed the raised contact angles they measured for acid-functionalised alkylsilane SAMs (when compared to acid-terminated alkylthiol SAMs on gold) to the presence of unreacted vinyl tail groups.[18] The general difficulties associated with the introduction of polar tail functionalities to alkylsilane-on-silica SAMs therefore mean that these monolayers do not represent an ideal basis for performing fundamental studies of cellular interactions with polar surfaces. Formation of alkylthiol-on-gold SAMs allows the preparation of pure, single-component polar surfaces and the preparation of mixed chemistries in a more precisely defined fashion, leading to a clearer understanding of differential cell–substratum responses.

Surface topography has also been used to direct cell growth. Clark and co-workers have examined the alignment of cells, on patterned fused quartz surfaces which were created using microelectronic fabrication techniques.[3,41] The results indicated that surface topography can be used to direct cell growth, but overall cellular response is strongly dependent on cell type, cell–cell interactions and the geometry of the patterns. The complicated fabrication procedure involved in creating these surfaces is a significant drawback to this approach to cell guidance. A study of growth cone guidance and neuron morphology on micropatterned laminin surfaces also required the use of complicated microfabrication procedures.[6]

Alkylthiol-on-gold SAM surfaces have been used previously to direct the growth of cells on a solid substratum,[42] but, in contrast to the present study, previous studies have utilised long-chain and complex alkanethiols, including oligo(ethylene glycol)-terminated alkylthiols. This study demonstrates that short-chain and readily available alkylthiols can be used in directing cell growth. A particular advantage is that the short-chain thiols require shorter processing times to create the patterns by photolithography. Work in this laboratory has highlighted that SAMs formed from short-chain adsorbates on gold are rapidly photo-oxidised while SAMs formed from adsorbates $HS(CH_2)_{n-1}CH_3$ ($n>10$) are photo-oxidised more slowly.[43] However, shorter chain thiols exhibit poorer order in the monolayers and it was not known whether using short-chain adsorbates to create the patterned substrates would result in adequate spatial definition for selectivity of biological response. The results of the present study clearly indicate that adequate differences in surface chemistry/cell response can be achieved using short-chain thiol compounds.

Our results indicate that the alkylthiol–gold system offers important advantages over other systems through the ease with which clean, precisely defined surface chemistries may be prepared. This system also provides an ideal basis for a study of the influence of various surface chemistries on cell attachment. Initial studies on other alkylthiol-on-gold systems suggest that surface energy may not be the dominating factor in determining cell adhesion. Other parameters may have an important role to play. For example, Sun *et al.* have demonstrated using FTIR–external reflectance spectroscopy that chain length is important in the interaction between self-assembled monolayers containing carboxylic acid terminal groups and vapour-phase *n*-alkylamine molecules.[44] The difference is attributed to the degree of structural order in the surface-confined acid group and resulting monolayer acidities. For example, mercaptoundecanoic acid displays significant hydrogen bonding within its COOH terminal groups whereas MPA has a disordered array of surface-confined COOH groups making it more susceptible to reaction with incoming molecules. Consequently, the less strongly hydrogen-bonded acid tail functionalities in the short-chain monolayer may undergo dissociation in aqueous media to yield the negatively charged carboxylate ion. Surface charge is thought to have a significant influence on cellular attachment and acid dissociation may therefore play a role in explaining the observed preference of 3T3 cells for MPA compared to OT.

The present study suffers from one main weakness: no attempt has been made to regulate the composition of the protein layer which adsorbs onto the SAM from the culture medium. A variety of proteins may be involved in regulating the cellular interactions with the SAM including, in particular, vitronectin and fibronectin. The sample surface chemistry influences the conformation of the adsorbed proteins, which is the critical factor in determining the cellular interactions of the SAM, and thus only indirectly influences cellular attachment. Systematic studies must attempt to examine the influence of surface chemistry on protein adsorption phenomena as the key to understanding cellular interactions. We are presently attempting to address this problem.

Conclusions

The rates of attachment of 3T3 fibroblasts to self-assembled monolayers formed by the adsorption of carboxylic acid- and methyl-terminated alkylthiols on gold have been studied. Approximately twice as many cells were found to attach to the acid-terminated monolayer than attached to the methyl-terminated monolayer. The fibroblasts exhibited a well spread morphology on the acid-terminated monolayer but were rounded and clustered together on the methyl-terminated monolayer. Differences were noted between our results and those of other authors who employed alkylsilane-on-silica SAMs, because of the attainment of higher surface energies for acid-terminated alkylthiol-on-gold SAMs. The importance of preparing well characterised model surfaces in studies of cell–surface interactions is emphasised. Patterned monolayers have also been produced and used to direct cell growth by creating spatially defined regions functionalised with MPA and surrounded by OT. Fibroblasts attached almost exclusively to regions functionalised by MPA. The morphologies of attached cells were found to be defined precisely by the geometry of the MPA-functionalised regions.

The authors are grateful to the Royal Society, the Leverhulme Trust (grant F114AY) and the EPSRC (grant GR/K28671) for their financial support, and to Jennifer C. Bussey for assistance with the SEM experiments.

References

1 D. M. Brunette, *Exp. Cell. Res.*, 1986, **164**, 11.
2 J. Meyle, A. F. von Recum, B. Gibbesch, W. Hutteman, U. Schlagenhauf and W. Schulte, *J. Appl. Biomater.*, 1991, **2**, 273.
3 P. Clark, P. Connolly, A. S. G. Curtis, J. A. T. Dow and C. D. W. Wilkinson, *J. Cell. Sci.*, 1991, **99**, 73.
4 T. Matsuda and T. Sugawara, *J. Biomed. Mater. Res.*, 1995, **29**, 749.
5 J. P. Ranieri, R. Bellamkonda, J. Jacob, T. G. Vargo, J. A. Gardella and P. Aebischer, *J. Biomed. Mater. Res.*, 1993, **27**, 917.
6 P. Clark, S. Britland and P. Connolly, *J. Cell Sci.*, 1993, **105**, 203.
7 K. Lewandowska, N. Balachander, C. N. Sukenik and L. A. Culp, *J. Cell. Physiol.*, 1989, **141**, 334.
8 K. Lewandowska, E. Pergament, C. N. Sukenik and L. A. Culp, *J. Biomed. Mater. Res.*, 1992, **26**, 1343.
9 S. Britland, P. Clark, P. Connolly and G. Moores, *Exp. Cell. Res.*, 1992, **198**, 124.
10 D. A. Stenger, J. H. Georger, C. S. Dulcey, J. J. Hickman, A. S. Rudolph, T. B. Nielsen, S. M. McCort and J. M. Clavert, *J. Am. Chem. Soc.*, 1992, **114**, 8435.
11 J. J. Hickman, S. K. Bhatia, J. N. Quong, P. Schoen, D. A. Stenger, C. J. Pike and C. W. Cotman, *J. Vac. Sci. Technol. A*, 1994, **12**, 607.
12 S. Margel, E. A. Vogler, L. Firment, T. Watt, S. Haynie and D. Y. Sogah, *J. Biomed. Mater. Res.*, 1993, **27**, 1463.
13 G. P. Lopez, M. W. Albers, S. L. Schreiber, R. Carroll, E. Peralta and G. M. Whitesides, *J. Am. Chem. Soc.*, 1993, **115**, 5877.
14 P. A. DiMilla, J. P. Folkers, H. A. Biebuyck, R. Harter, G. P. Lopez and G. M. Whitesides, *J. Am. Chem. Soc.*, 1994, **116**, 2225.
15 M. D. Porter, T. B. Bright, D. L. Allara and C. E. D. Chidsey, *J. Am. Chem. Soc.*, 1987, **109**, 3559.
16 R. G. Nuzzo, B. R. Zegarski and L. H. Dubois, *J. Am. Chem. Soc.*, 1987, **109**, 733.
17 C. D. Bain, E. B. Troughton, Y-T. Tao, J. Evall, G. M. Whitesides and R. G. Nuzzo, *J. Am. Chem. Soc.*, 1989, **111**, 321.
18 S. R. Wasserman, Y-T. Tao and G. M. Whitesides, *Langmuir*, 1989, **5**, 1074.
19 C. D. Bain and G. M. Whitesides, *J. Am. Chem. Soc.*, 1989, **111**, 7164.
20 P. E. Laibinis, R. G. Nuzzo and G. M. Whitesides, *J. Phys. Chem.*, 1992, **96**, 5097.
21 J. P. Folkers, P. E. Laibinis, G. M. Whitesides and J. Deutch, *J. Phys. Chem.*, 1994, **98**, 563.
22 H. A. Biebuyck and G. M. Whitesides, *Langmuir*, 1994, **10**, 4581.
23 D. A. Offord and J. H. Griffin, *Langmuir*, 1993, **9**, 3015.
24 M. J. Tarlov, *Langmuir*, 1992, **8**, 80.
25 D. R. Jung and A. W. Czanderna, *Crit. Rev. Solid State Mater. Sci.*, 1994, **19**, 1.
26 D. J. Dunaway and R. L. McCarley, *Langmuir*, 1994, **10**, 3598.
27 T. A. Jones, G. P. Perez, B. J. Johnson and R. M. Crooks, *Langmuir*, 1995, **11**, 1318.
28 O. Chailapakul and R. M. Crooks, *Langmuir*, 1995, **11**, 1329.
29 K. D. Schierbaum, T. Weiss, E. U. Thoden van Velzen, J. F. J. Engbersen, D. N. Reinhoudt and W. Gopel, *Science*, 1994, **265**, 1413.
30 R. Reiter, H. Motschmann and W. Knoll, *Langmuir*, 1993, **9**, 2430.
31 K. L. Prime and G. M. Whitesides, *Science*, 1991, **252**, 1164.
32 P. Tengvall, M. Lestelius, B. Liedberg and I. Lundstrom, *Langmuir*, 1992, **8**, 1236.
33 M. Lestelius, B. Liedberg, I. Lundstrom and P. Tengvall, *J. Biomed. Mater. Res.*, 1994, **28**, 871.
34 M. J. Tarlov, D. R. F. Burgess and G. Gillen, *J. Am. Chem. Soc.*, 1993, **115**, 5305.
35 G. Gillen, J. Bennett, M. J. Tarlov and D. R. F. Burgess, *Anal. Chem.*, 1994, **66**, 2170.
36 M. R. Alexander, P. V. Wright and B. D. Ratner, *Surf. Interface Anal.*, 1996, **24**, 217.
37 E. W. Wollman, C. D. Frisbie and M. S. Wrighton, *Langmuir*, 1995, **9**, 1517.
38 G. P. Lopez, H. A. Biebuyck and G. M. Whitesides, *Langmuir*, 1993, **9**, 1513.
39 K. E. Healy, C. H. Thomas, A. Rezania, J. E. Kim, P. J. McKeown, B. Lom and P. E. Hockberger, *Biomaterials*, 1996, **17**, 195.
40 E. Cussen, R. Wiggs, D. A. Hutt, G. J. Leggett and T. L. Parker, unpublished results.
41 P. Clark, P. Connolly and G. R. Moores, *J. Cell Sci.*, 1992, **103**, 287.
42 R. Singhvi, A. Kumar, G. P. Lopez, G. N. Stephanopoulos, D. I. C. Wang, G. M. Whitesides and D. E. Ingber, *Science*, 1994, **264**, 696.
43 D. A. Hutt and G. J. Leggett, *J. Phys. Chem.*, 1996, **100**, 6657.
44 L. Sun, R. M. Crooks and A. J. Ricco, *Langmuir*, 1993, **9**, 1775.

Paper 6/07204F; *Received* 22*nd October*, 1996